The Astrophysical Journal, 643:1151–1159, 2006 June 1

NGC 6791: AN EXOTIC OPEN CLUSTER OR THE NUCLEUS OF A TIDALLY DISRUPTED GALAXY?

Giovanni Carraro[1,2]
Astronomy Department, Yale University, New Haven, CT 06520-8101; gcarraro@das.uchile.cl

Sandro Villanova
Dipartimento di Astronomia, Università di Padova, vicolo Osservatorio 2, I-35122 Padova, Italy; villanova@pd.astro.it

Pierre Demarque and M. Virginia McSwain[3]
Astronomy Department, Yale University, New Haven, CT 06520-8101; demarque@astro.yale.edu, mcswain@astro.yale.edu

Giampaolo Piotto
Dipartimento di Astronomia, Università di Padova, vicolo Osservatorio 2, I-35122 Padova, Italy; piotto@pd.astro.it

and

Luigi R. Bedin
European Southern Observatory, Karl-Schwarzschildstrasse 2, 85748 Garching, Germany; lbedin@eso.org
Received 2005 October 13; accepted 2005 December 29

ABSTRACT

We report on high-resolution echelle spectroscopy of 20 giant stars in the Galactic old open cluster NGC 6791, obtained with Hydra at the WIYN telescope. High-precision radial velocity allows us to isolate 15 bona fide cluster members. From 10 of them we derive a global $[M/H] = +0.39 \pm 0.05$. We therefore confirm that NGC 6791 is extremely metal-rich, exhibits a few marginally subsolar abundance ratios, and within the resolution of our spectra does not show evidence of spread in metal abundance. With these new data we rederive the fundamental cluster parameters, suggesting that it is about 8 Gyr old and 4.3 kpc from the Sun. The combination of its chemical properties, age, position, and Galactic orbit hardly makes NGC 6791 a genuine Population I open cluster. We discuss possible interpretations of the cluster peculiarities, suggesting that the cluster might be what remains of a much larger system whose initial potential well could have been sufficient to produce high-metallicity stars and which has been depopulated by the tidal field of the Galaxy. Alternatively, its current properties may be explained by the perturbation of the Galactic bar on an object that originated well inside the solar ring, where the metal enrichment was very fast.

Subject headings: open clusters and associations: general — open clusters and associations: individual (NGC 6791)

1. INTRODUCTION

NGC 6791 is an extremely interesting and intriguing open cluster. The combination of old age, small distance, and high metal abundance makes this cluster very attractive, and indeed in the last 40 years it has been the target of intensive and numerous studies (Carney et al. 2005 and references therein). A large number of optical photometric studies (Stetson et al. 2003 and references therein) have been recently complemented by the deep *Hubble Space Telescope* (*HST*) Advanced Camera for Surveys (ACS) investigation by King et al. (2005) and the near-IR study by Carney et al. (2005).

Since the pioneering study of Kinman (1965) it was clear that NGC 6791 is a very old and very metal-rich cluster. Its age was measured several times by using different sets of isochrones (Carraro et al. 1999 and references therein), and it is probably confined in the range 8–12 Gyr, depending on the cluster's precise metal abundance. Taylor (2001 and references therein) critically reviewed all the available metallicity estimates, concluding that the [Fe/H] for NGC 6791 should probably lie in the range +0.16 to +0.44 dex. This combination of age and metallicity is unique in the Milky Way open cluster population and has been recently questioned by Bedin et al. (2005), whose *HST* study of the white dwarf cooling sequence supports a much younger age. As these authors comment, this age discrepancy may arise from defects in the current white dwarf models or from the cluster's poorly known metal abundance.

It is interesting to note that the cluster is also known to harbor a number of sdB/sdO stars (Landsman et al. 1998; Buson et al. 2006), which may be explained by a scenario of a high-metallicity-driven wind in the red giant branch (RGB) phase of the progenitors of these stars or, more simply, by the binarity hypothesis (Green et al. 2005). The UV upturn (namely, the abrupt rise in the UV continuum emission shortward of $\lambda \approx 2000$ Å) similar to that typical of any elliptical galaxy (Landsman et al. 1998) and the highly eccentric orbit, unusual for a Population I object, make this cluster even more intriguing.

In an attempt to substantially improve our knowledge of NGC 6791, we carried out a spectroscopic campaign to provide radial velocities and accurate metallicities of a statistically significant number of stars in the cluster. In fact, current abundance determinations either lack sufficient resolution or are restricted to a very small number of stars. This new set of abundance estimates coupled with the high quality of existing photometry (Stetson et al. 2003) allow us to significantly improve on the fundamental parameters of this cluster and better clarify its intriguing nature.

2. OBSERVATIONS

The observations were carried out on the night of 2005 July 28 with the Hydra spectrograph at the Wisconsin Indiana Yale NOAO

[1] Also at Departamento de Astrónomia, Universidad de Chile, Casilla 36-D, Santiago de Chile, Chile.
[2] Andes Fellow; on leave from Dipartimento di Astronomia, Università di Padova, vicolo Osservatorio 2, I-35122 Padova, Italy.
[3] NSF Astronomy and Astrophysics Postdoctoral Fellow.

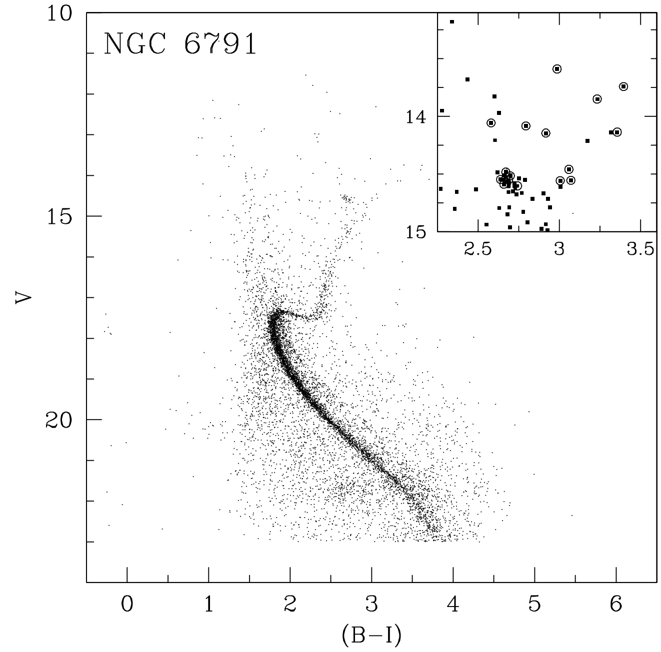

FIG. 1.—CMD of NGC 6791 (from Stetson et al. [2003] photometry). The inset shows the position of the observed stars.

(WIYN) telescope at Kitt Peak observatory under photometric conditions and typical seeing of 1.″1. The Multi-Object Spectrograph (MOS) consists of the Hydra positioner, which in 20 minutes can place 89 fibers within the 1° diameter focal plane of the telescope to ≈0.″2 precision. This project employed the 3″ diameter red-optimized fiber bundle. The fibers feed a bench-mounted spectrograph in a thermally isolated room. With the echelle grating and the Bench Spectrograph Camera, the system produces a resolution of 20,000 at 6000 Å. The wavelength coverage of 200 Å around the central wavelength of 6000 Å provides a rich array of narrow absorption lines. We observed 20 RGB/clump stars (see Fig. 1) with 45 minute exposures, for a grand total of 4.5 hr of actual photon collection time on the same single star. The 20 stars were selected from the Stetson et al. (2003) photometric catalog to be giant stars and to have the right magnitudes to be observed with the WIYN 3.6 m telescope. We restricted the sample to giant stars brighter than $V \approx 15$. The stars are listed in Table 1, where column (1) reports Stetson et al. (2003) numbering, and column (2) gives Kinman (1965) numbering. Then coordinates, magnitudes, and colors were taken from Stetson et al. (2003). The radial velocities and spectral classification have been derived in this paper, following Villanova et al. (2004).

3. DATA REDUCTION

Images were reduced using IRAF,[4] including bias subtraction, flat-field correction, frame combination, extraction of spectral orders, wavelength calibration, sky subtraction, and spectral rectification. The single orders were merged into a single spectrum. As an example, we show in Figure 2 a portion of the reduced, normalized spectrum for star 11814, for which some spectral lines are identified. Some spectra have a very low signal-to-noise ratio (S/N), although all the observed stars have practically the same magnitude. This could happen for two reasons: the first one is an imperfect pointing of the fiber, and the second one is a possible bad fiber transmission. Because of this, we could not use five stars for abundance measurements (see below).

4. RADIAL VELOCITIES

Radial velocities (RVs) for RGB and clump stars in NGC 6791 have been determined many times in the past. Kinman (1965) obtained radial velocities for 19 stars, and spectral types

[4] IRAF is distributed by the National Optical Astronomy Observatory, which is operated by the Association of Universities for Research in Astronomy, Inc., under cooperative agreement with the National Science Foundation.

TABLE 1
Observed Stars

ID (1)	Kinman (1965) Numbering (2)	R.A. (J2000.0) (3)	Decl. (J2000.0) (4)	V (5)	$B-I$ (6)	V_{rad} (km s^{-1}) (7)	S/N (8)	Spectral Type (9)
10898	. . .	19 21 01.13	+37 42 13.80	14.459	3.059	−47.37 ± 0.088	40	K4 III
11814	3003	19 21 04.27	+37 47 18.90	13.849	3.233	−46.52 ± 0.082	60	K4/5 III
1442	. . .	19 21 16.33	+37 52 15.80	14.056	2.580	−11.84 ± 0.056	100	. . .
2044	. . .	19 20 30.92	+37 48 45.30	14.144	2.917	−5.27 ± 0.072	40	. . .
2423	. . .	19 20 33.26	+37 50 12.70	14.082	2.794	−220.41 ± 0.066	70	. . .
2793	3036	19 20 34.86	+37 46 30.10	14.538	2.751	−48.00 ± 0.108	30	M1/2 III
3369	3030	19 20 37.89	+37 44 49.30	14.529	2.673	−48.37 ± 0.094	40	K2/3 III
4162	. . .	19 20 40.85	+37 46 21.80	14.551	2.687	−52.11 ± 0.146	10	K2/3 III
4715	. . .	19 20 42.73	+37 51 07.70	14.515	2.698	−47.91 ± 0.088	50	K2/3 III
5583	. . .	19 20 45.58	+37 39 51.20	14.602	2.742	−43.62 ± 0.196	10	K3/4 III
6940	3013	19 20 49.67	+37 44 08.00	14.588	2.659	−46.00 ± 0.155	10	K2/3 III
7922	. . .	19 20 52.47	+37 50 15.80	14.482	2.671	−48.28 ± 0.080	30	K2/3 III
7972	3010	19 20 52.60	+37 44 28.50	14.136	3.356	−44.35 ± 0.094	40	K7 III
8082	SE-49	19 20 52.89	+37 45 33.40	14.546	2.639	−46.18 ± 0.102	40	K2/3 III
8266	2001	19 20 53.39	+37 48 28.40	13.741	3.395	−47.73 ± 0.080	40	K9 III
852	. . .	19 20 22.40	+37 51 42.40	14.738	2.748	−67.91 ± 0.267	10	. . .
8563	. . .	19 20 54.19	+37 46 28.80	14.554	3.071	−42.44 ± 0.084	40	K4 III
8904	2008	19 20 55.11	+37 47 16.50	13.862	3.603	−46.91 ± 0.098	30	M0 III
8988	3018	19 20 55.31	+37 43 15.60	14.557	3.005	−47.46 ± 0.088	30	K4 III
95	. . .	19 20 11.19	+37 49 48.70	13.589	2.986	−72.93 ± 0.076	50	. . .

Note.—Units of right ascension are hours, minutes, and seconds, and units of declination are degrees, arcminutes, and arcseconds.

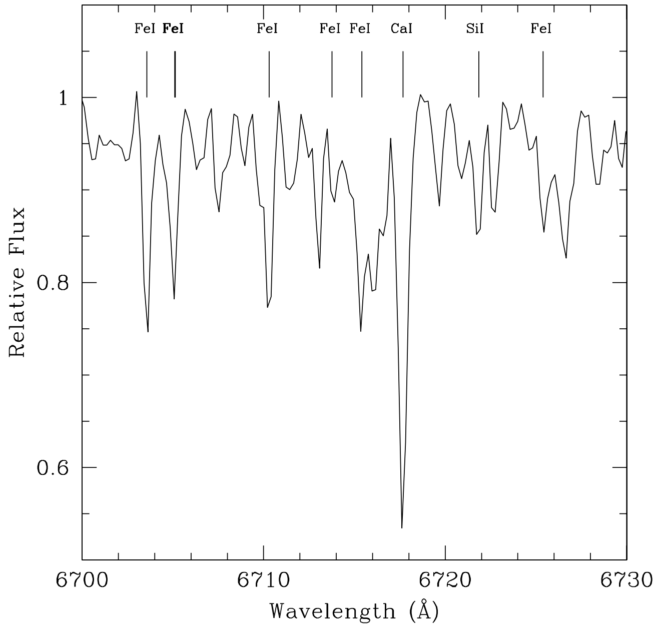

FIG. 2.—Example of the extracted spectrum for star 11814, with the main lines indicated.

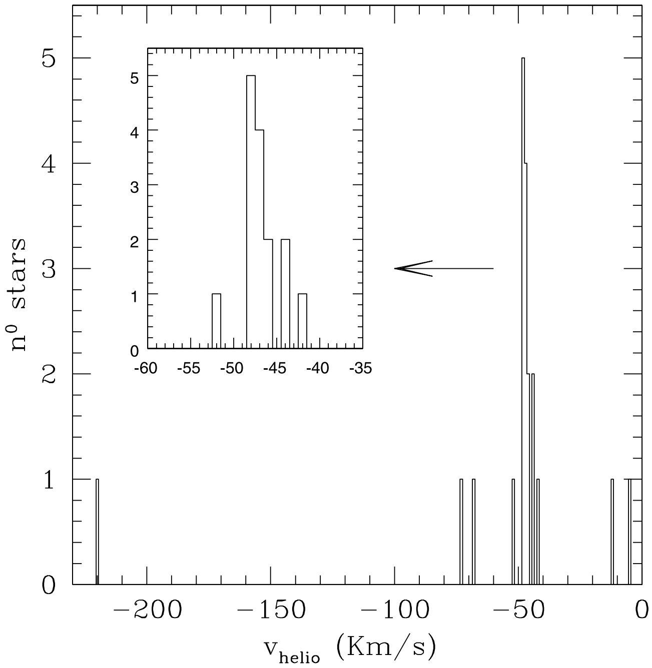

FIG. 3.—Radial velocity distribution of the 20 observed target stars.

for 21. Later, RVs were measured by Geisler (1988; 12 stars), Friel et al. (1989; 9 stars), Garnavich et al. (1994; 18 stars), Scott et al. (1995; 32 stars), and Friel et al. (2002; 41 stars), with different resolution and precision.

We derived here RVs for 20 stars (see Table 1). The radial velocities of the target stars were measured using the IRAF `fxcor` task, which cross-correlates the object spectrum with a template. As a template, we used a synthetic spectrum calculated by SPECTRUM (see § 5.2 for a description of the program) with roughly the same atmospheric parameters and metallicity of the observed stars. The final error in the radial velocities was typically less than 0.2 km s^{-1}, and in many cases less than 0.1 km s^{-1}. These errors are significantly lower than in any other previous investigation. This allowed us to clean out field interlopers and isolate 15 bona fide members. RVs are plotted in Figure 3. Five stars have radial velocities completely different from the others, and so were considered nonmembers, although it is possible that some of them are binary stars.

A few of our targets are in common with previous investigations, and we can have an external check on our RV measurements. For 11 stars, we provide the first estimate of the RV. In general, we find that Garnavich et al. (1994) RV estimates (for stars 3003, 3010, 3036, 2001, 3018, and 2008) are systematically larger than ours by about 5–7 km s^{-1}, although, given their typical large error (5–15 km s^{-1}), these differences cannot be considered statistically significant. Also, Kinman (1965) RVs for the two stars in common with our investigation (stars 2001 and 2008) are larger than our estimate. The largest deviation is with respect to the RVs by Friel et al. (2002) and their previous measurements (Scott et al. 1995; Friel et al. 1989). In this case, some differences exceed 20 km s^{-1} (stars 3003 and 2008). Finally, within the errors, we find a good agreement for the two stars (stars 3003 and 3010) we have in common with Geisler (1988).

From the RVs of the 15 cluster members in our sample, we obtain a mean radial velocity $V_r = -47.1 \pm 0.8$ km s^{-1}, in good agreement, within the errors, with the values obtained by the other authors, with the exception of Kinman (1965). The RV dispersion is thus $\sigma_r = 2.2 \pm 0.4$ km s^{-1}.

5. ABUNDANCE ANALYSIS

5.1. *Atmospheric Parameters*

The atmospheric parameters (see Table 2) were obtained from the photometric BVI_C data of Stetson et al. (2003). According to Stetson et al., the most likely reddening and absolute distance modulus are $E(B-V) = 0.09$ $[E(V-I) = 0.11]$ and $(m-M)_0 = 12.79$. Effective temperatures ($T_{\rm eff}$) were obtained from the color $T_{\rm eff}$ relations of Alonso et al. (1999), Sekiguchi & Fukugita (2000), and Ramirez & Melendez (2005). The temperatures, obtained from the $B-V$ and $V-I$ colors using the quoted relations, are in agreement within 50–100 deg K. The gravity $\log(g)$ was derived from the canonical formula $\log(g/g_\odot) = 4\log(T_{\rm eff}/T_\odot) - \log(L/L_\odot) + \log(M/M_\odot)$. In this equation, the mass $M/M_\odot$ was derived from Straizys & Kuriliene (1981). The luminosity $L/L_\odot$ was derived from the absolute magnitude M_V,

TABLE 2
ADOPTED ATMOSPHERIC PARAMETERS

ID	$T_{\rm eff}$ (deg K)	log g (dex)	v_t (km s^{-1})
10898	4100	2.53	1.0
11814	3980	2.17	1.1
2793	3760	2.02	1.1
3369	4400	2.79	1.0
4162	4370	2.78	1.0
4715	4360	2.76	1.0
5583	4300	2.75	1.0
6940	4400	2.81	1.0
7922	4390	2.77	1.0
7972	3920	2.23	1.1
8082	4410	2.81	1.0
8266	3900	2.04	1.2
8563	4080	2.55	1.0
8904	3830	2.01	1.2
8988	4130	2.60	1.0

TABLE 3

Line List

Line and Identification				
6408.016 Fe I	6411.650 Fe I	6419.980 Fe I	6421.350 Fe I	6436.430 Fe I
6439.075 Ca I	6449.808 Ca I	6455.598 Ca I		6464.661 Fe I
6469.123 Fe I	6469.210 Fe I	6471.662 Ca I		6481.880 Fe I
6491.561 Ti II	6494.980 Fe I	6496.897 Ba II		6498.950 Fe I
6499.650 Ca I	6501.691 Ti I	6518.380 Fe I	6527.202 Si I	Ni I
6554.230 Ti I	6556.070 Ti I	6569.230 Fe I	6572.779 Ca I	6574.240 Fe I
6575.020 Fe I	6581.221 Fe I	6593.880 Fe I	6606.970 Ti ıI	6608.030 Fe I
6609.120 Fe I	6625.041 Fe I	6627.560 Fe I	6633.440 Fe I	6633.760 Fe I
6634.100 Fe I	6643.640 Ni I	6646.980 Fe I	6663.231 Fe I	6663.450 Fe I
6677.955 Fe I	6677.990 Fe I	6698.673 Al I	6703.570 Fe I	6705.101 Fe I
6705.131 Fe I	6710.310 Fe I	6713.760 Fe I	6715.410 Fe I	6717.681 Ca I
6721.848 Si I	6725.390 Fe I	6733.160 Fe I	6737.980 Fe I	6741.628 Si I
6743.120 Ti I	6743.185 Ti I	6750.150 Fe I		

adopting the distance modulus of Stetson et al. (2003). The bolometric correction (BC) was derived from the BC-$T_{\rm eff}$ relation from Alonso et al. (1999). The typical error in $\log(g)$ is 0.1 dex.

Finally, the adopted microturbulence velocity is the mean of the values given by the relation $v_t = (1.19\times10^{-3})T_{\rm eff} - 0.90\log(g) - 2$ (Gratton et al. 1996) and $v_t = 2.22 - 0.322\log(g)$. The typical error in v_t is 0.1 km s^{-1}.

5.2. *Abundance Determination*

The resolution ($R = 17{,}000$ at 6580 Å) of our spectra, the high metallicity of the cluster, and the low temperature of the target stars cause a lot of blending, and therefore it was not possible to measure the equivalent width of the single spectral lines. For this reason, the abundances were determined by comparing the observed spectra with synthetic ones. The synthetic spectra were calculated by running SPECTRUM, the local thermodynamical equilibrium (LTE) spectral synthesis program freely distributed by Richard O. Gray (see Piotto et al. [2005] for the details on our synthetic spectra calculation). Model atmospheres were interpolated from the grid of Kurucz (1992) models by using the values of $T_{\rm eff}$ and $\log(g)$ determined as explained in § 5.1. We analyzed stars with $T_{\rm eff} > 3900$ deg K because, for lower temperatures, molecular bands were present, creating difficulties for continuum determination. We analyzed only 10 stars, after rejecting the nonmembers and the stars that were too faint and too cool.

First of all, we compared the entire spectrum (range 6400–6760 Å) with the synthetic one in order to obtain an estimate of the global metallicity [M/H]. Then, we analyzed single lines in order to measure abundances of Fe, Ca, Ti, Ba, Al, Ni, and Si.

A preliminary line list was obtained considering all the strongest lines present in our spectra, identified using the line list distributed with SPECTRUM. The final line list was created from the preliminary one by comparing the observed solar spectrum with a synthetic one, calculated with SPECTRUM for the Sun parameters [$T_{\rm eff} = 5777$ K, $\log(g) = 4.44$, $v_t = 0.8$ m s^{-1}]. The lines in the synthetic spectrum that did not properly match the observed ones were rejected. We also checked whether the preliminary line identification was correct, using the MOORE line database (Moore et al. 1996). Table 3 shows the final list of lines we used in our analysis. The resulting metallicities for each star are listed in Table 4.

Due to the radial velocity shift, a few lines (6462.567, 6475.630, 6493.781, and 6532.890 Å) overlapped with telluric lines. We did not consider these lines in the abundances determination.

An example of the comparison between synthetic and observed spectra is shown in Figure 4, for the case of star 11814. Finally, using the stellar parameters [colors, $T_{\rm eff}$, and $\log(g)$] and the absolute calibration of the MK system (Straizys & Kuriliene 1981), for each star we derived the stellar spectral classification (see Villanova et al. [2004] for details), which is listed in column (9) of Table 1.

The weighted mean of the [Fe/H] content of the 10 members of NGC 6791 analyzed in the present paper is $[\mathrm{Fe/H}] = +0.39 \pm 0.01$ (internal error). Previous investigations reported a variety of estimates for the metallicity of NGC 6791. By using low-resolution spectroscopy, Friel & Janes (1993) obtained $[\mathrm{Fe/H}] = +0.19 \pm 0.19$ from 9 stars, and Friel et al. (2002) obtained $[\mathrm{Fe/H}] = +0.11 \pm 0.10$ from moderate-resolution spectra of 39 stars. Because of the large errors, the first estimate is

TABLE 4

Mean Stellar Abundances

ID	[M/H]	[Fe/H]	[Ca I/H]	[Ti/H]	[Ba/H]	[Si/H]	[Ni/H]	[Al/H]
10898	0.37 ± 0.06	0.38 ± 0.08	0.33 ± 0.12	0.38 ± 0.02	...	0.42	0.32	0.20
11814	0.39 ± 0.09	0.34 ± 0.08	0.32 ± 0.08	0.34 ± 0.05	...	0.39 ± 0.03	0.29 ± 0.14	0.23
3369	0.41 ± 0.09	0.37 ± 0.09	0.35 ± 0.05	0.38 ± 0.07	0.19	0.42	0.36	0.18
4715	0.39 ± 0.07	0.36 ± 0.05	0.33 ± 0.07	0.35 ± 0.02	0.18	0.41 ± 0.02	0.42	0.23
7922	0.39 ± 0.02	0.39 ± 0.07	0.33 ± 0.14	0.36 ± 0.02	...	0.37 ± 0.09	0.40	0.22
7972	0.40 ± 0.09	0.39 ± 0.05	0.35 ± 0.06	0.34 ± 0.05	0.20	0.39	0.41	0.26
8082	0.42 ± 0.04	0.38 ± 0.05	0.38 ± 0.07	0.38 ± 0.07	0.14	0.36	0.48	0.23
8266	0.37 ± 0.05	0.37 ± 0.05	0.38 ± 0.07	0.37	0.24	0.39	0.31	0.19
8563	0.38 ± 0.08	0.38 ± 0.06	0.32 ± 0.03	0.36 ± 0.04	0.32	0.42	0.37	0.25
8988	0.36 ± 0.06	0.40 ± 0.07	0.35 ± 0.10	0.31 ± 0.07	0.22	0.39	0.34	...

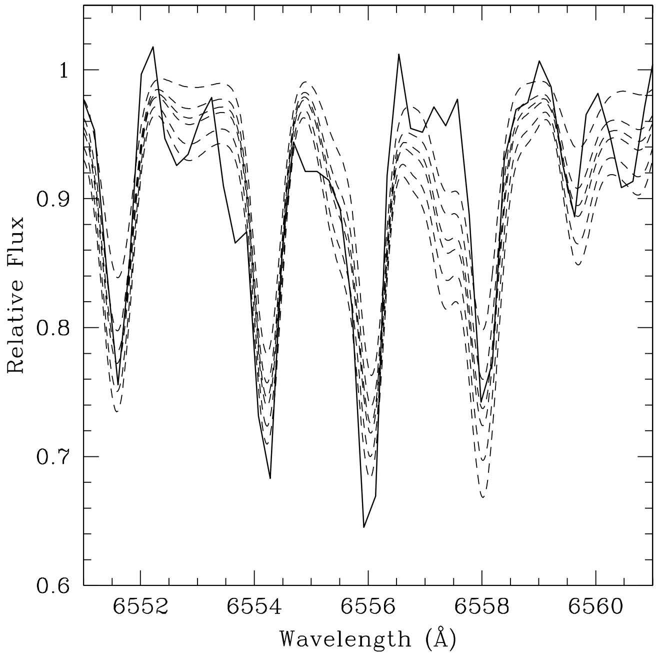

FIG. 4.—Spectrum of Fig. 2 (*thick line*) and a set of synthetic spectra for $[M/H] = -0.2$, 0.0, +0.2, +0.5, and +0.7, from top to bottom.

compatible with ours, within 1 σ, while the second one is off by almost 3 σ.

Interestingly enough, our results are in very good agreement with the study by Peterson & Green (1998), who derived $[Fe/H] = +0.40 \pm 0.10$ for star 2017, a cool blue horizontal branch star, using a resolution very similar to the one used in the present study.

In conclusion, our results confirm that NGC 6791 is actually a very metal-rich cluster. It is interesting to note that within the errors of our measurements, the metallicities listed in Table 4 do not show any significant abundance spread.

5.3. *Abundance Ratios*

Abundance ratios constitute a powerful tool to assign a cluster to a stellar population (Friel et al. 2003; Carraro et al. 2004; Villanova et al. 2005). In Table 5 we list the abundance ratios for the observed stars in NGC 6791. These values do not show any particular anomaly. All the abundance ratios are solar scaled, with the exception of [Al/Fe] and [Ba/Fe], which seem to be slightly underabundant. Our ratios are in good agreement with those provided by Peterson & Green (1998).

6. DISTANCE AND AGE OF NGC 6791

Our accurate determination of the metal content of NGC 6791 allows a new, more reliable estimate of the cluster distance and age. To this purpose, here we fit the observed color magnitude diagram (CMD) from Stetson et al. (2003) with both the Padova (Girardi et al. 2000) and Yale-Yonsei isochrones (Yi et al. 2001; Demarque et al. 2004). Previous similar studies allowed us to confine the cluster age in the relatively large interval between 8 and 12 Gyr (Carraro et al. 1994; Chaboyer et al. 1999; King et al. 2005; Carney et al. 2005 and references therein). As discussed in Stetson et al. (2003) and confirmed in this work, the cluster reddening is $E(B-V) = 0.09 \pm 0.04$. There is a large scatter in the literature on the absolute distance modulus $(m-M)_0$ estimates, which range in the interval between 12.6 and 13.6. These large uncertainties in both age and distance have been usually ascribed to uncertainties in the cluster metal abundance. The new spectroscopic data presented in this paper allow us to put these fundamental parameters on a more solid basis.

6.1. *Padova Isochrones*

Our $[Fe/H] = 0.39$ empirical measurement translates into a metallicity $Z = 0.046$ (Carraro et al. 1999) and implies a $\Delta Y/\Delta Z$ close to 2. We generated isochrones for this metallicity and for ages ranging from 7 to 11 Gyr from Girardi et al. (2000). An appropriate and meaningful isochrone fit implies that all the loci of the CMD—e.g., the turnoff (TO) point, the subgiant branch (SGB), the RGB, and the clump of He-burning stars—must be simultaneously overlapped by the models. Our best-fit estimate (by eye) is shown in Figures 5 and 6, both in the V versus $(B-V)$ and V versus $(V-I)$ plane. In Figure 5 we plot the V versus $(B-V)$ CMD of NGC 6791 and superpose the whole set of isochrones, whereas in Figure 6 we only show the best-fit isochrone in the V versus $(B-V)$ and V versus $(V-I)$ plane.

The isochrone solutions in Figure 5 have been obtained by shifting the theoretical lines by $E(B-V) = 0.09$ and $(m-M)_V = 13.35$. Clearly, ages older than 9 Gyr can be ruled out, since a fit to the TO with an older isochrone implies a decrease to the distance modulus, but, in this way, the theoretical clump would be brighter than the observed one. On the other hand, ages younger than 8 Gyr do not seem possible, since a fit of the TO region with a younger isochrone would result in a RGB redder than the observed one (implying a reddening value significantly larger that the observational limits), and also the clump magnitude would be fainter than the observed counterpart.

Only the isochrones for ages of 8 and 9 Gyr provide a good fit. Specifically, the 9 Gyr isochrone fits well the CMD with the

TABLE 5
ABUNDANCE RATIOS

ID	[Fe/H]	[Ca/Fe]	[Ti/Fe]	[Ba/Fe]	[Si/Fe]	[Ni/Fe]	[Al/Fe]
10898	0.38 ± 0.08	−0.05	0.00	...	+0.04	−0.06	−0.18
11814	0.34 ± 0.08	−0.02	0.00	...	+0.05	−0.05	−0.11
3369	0.37 ± 0.09	−0.02	+0.01	−0.14	+0.05	−0.01	−0.19
4715	0.36 ± 0.05	−0.03	−0.01	−0.15	+0.05	+0.06	−0.13
7922	0.39 ± 0.07	−0.06	−0.03	...	−0.02	+0.01	−0.17
7972	0.39 ± 0.05	−0.04	−0.05	−0.15	0.00	+0.02	−0.13
8082	0.38 ± 0.05	0.00	0.00	−0.22	−0.02	−0.02	−0.15
8266	0.37 ± 0.05	+0.01	0.00	−0.12	+0.02	+0.02	−0.18
8563	0.38 ± 0.06	−0.06	−0.06	0.00	+0.04	−0.01	−0.13
8988	0.40 ± 0.07	−0.05	−0.06	−0.13	−0.01	−0.01	...

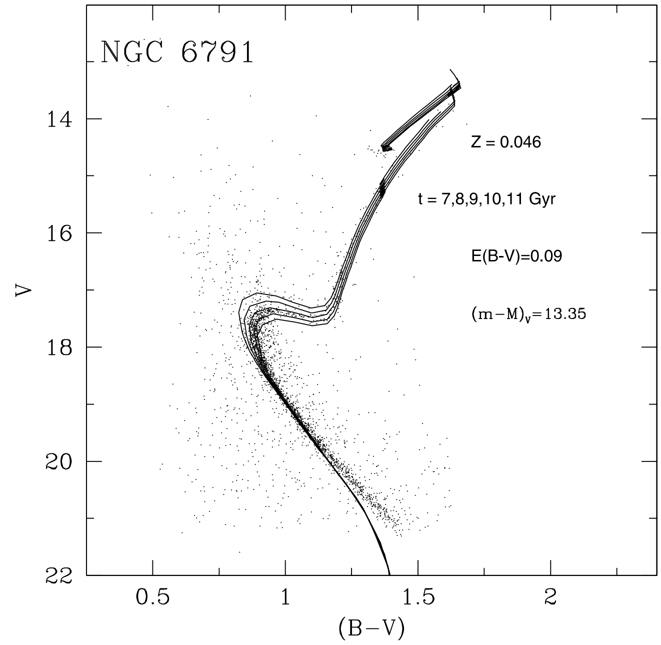

FIG. 5.—Five Padova isochrones for the ages of 7, 8, 9, 10, and 11 Gyr, fitted to the observed CMD in the V vs. $(B-V)$ plane. The isochrones are shifted by $E(B-V) = 0.09$ and $(m-M)_v = 13.35$.

adopted parameters, although the clump luminosity turns out to be slightly brighter than the observed one. On the other hand, the 8 Gyr isochrone must be shifted by $E(B-V) = 0.09$ and $(m-M)_V = 13.45$ to provide a very good fit. This is shown in Figure 6. We note that the lower main sequence (MS) is mismatched. This is a well-known problem for metal-rich clusters, as extensively discussed by Bedin et al. (2001), and it is likely due to problems in the transformation of the models from the theoretical to the observational plane.

Overall, however, the fit is very good, and implies for NGC 6791 this set of fundamental parameters: 8.0 ± 1.0 Gyr, 13.07 ± 0.05 (internal error), and 0.09 ± 0.01 for the age, absolute distance modulus, and reddening, respectively. The associated errors are internal errors and have been estimated by eye. They simply reflect the degree of freedom we have to displace the isochrones while still achieving an acceptable fit.

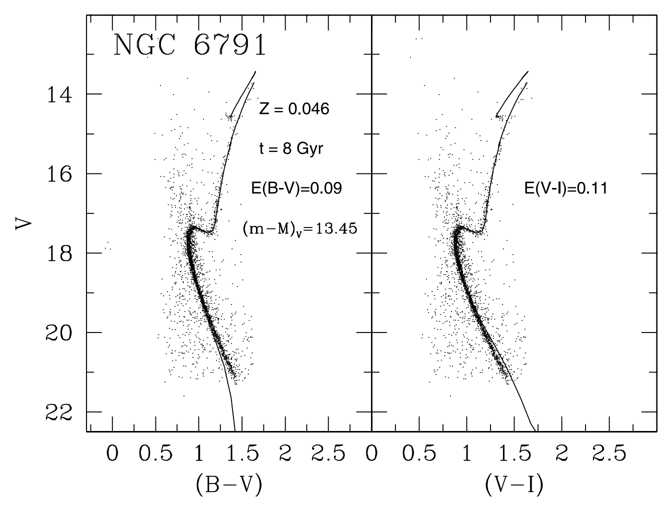

FIG. 6.—Best-fit isochrone solution of the CMD of NGC 6791 with the Padova models. The isochrone and setting parameters are indicated in the plot.

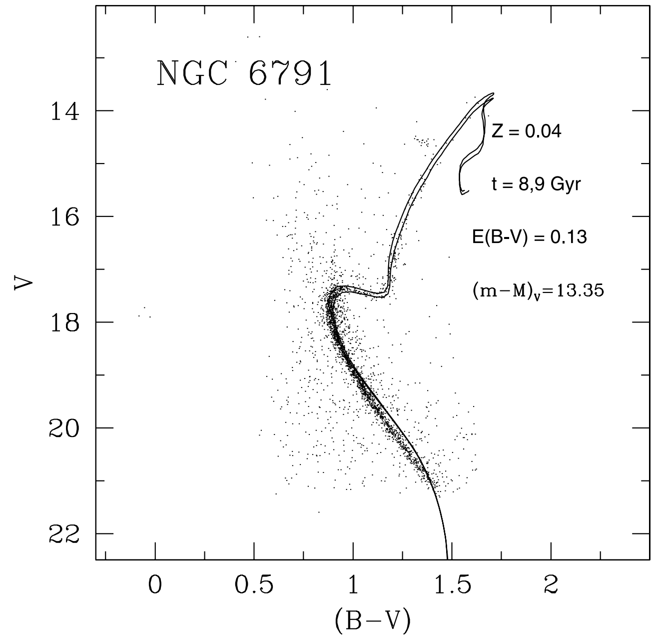

FIG. 7.—Yale-Yonsei isochrone solution for ages of 8 and 9 Gyr.

6.2. *Yale-Yonsei Isochrones*

An independent determination of the age, distance, and a constraint on the reddening of NGC 6791 can be derived using the Y^2 isochrones (Yi et al. 2001; Demarque et al. 2004). The Padova and Y^2 isochrones were both constructed using the same OPAL opacity tables. Otherwise, the description of the microscopic and macroscopic physics, as well as the numerical procedures, differ in many details in the two sets of isochrones. The color transformations are also independently derived.

In the Y^2 system, in which $Z_\odot = 0.0181$, $[\mathrm{Fe/H}] = 0.39$ corresponds to $(Y, Z) = (0.31, 0.04)$. The fit is based on the MS position just below the TO, the position of the TO point, the SGB, and the RGB color. A good fit, as shown in Figure 7, is obtained for $(m-M)_V = 13.35$, 0.1 mag smaller than the distance modulus we used for the Padova isochrone fit. The best fit is obtained by assuming a reddening $E(B-V) = 0.13$, somewhat larger than the reddening adopted in § 6.1, but still within the estimated range of previous investigations. The age we derive from the Y^2 fit is between 8 and 9 Gyr, in good agreement with the Padova age, although one notes that the position of the lower MS differs in the two sets of isochrones. The unevolved MS of the Padova isochrones has a steeper downward slope than the observations, whereas the opposite holds for the Y^2 isochrones.

Similarly, Chaboyer et al. (1999) concluded that the cluster age is 8.0 ± 0.5 Gyr, assuming $[\mathrm{Fe/H}] = 0.4$, but using an older observational data set (Kaluzny & Rucinski 1995) and a version of the Yale stellar evolution code that slightly differs from the one used to construct the Y^2 isochrones. In an analysis of their infrared photometry, Carney et al. (2005) derived an age between 9 Gyr (for $[\mathrm{Fe/H}] = 0.3$) and 7.5 Gyr (for $[\mathrm{Fe/H}] = 0.5$), also in good agreement with our result. Both the Chaboyer et al. (1999) and the Carney et al. (2005) ages are consistent with the Padova and Y^2 fits described in this paper. We should note, however, that the Carney age estimates were obtained using the same set of Y^2 isochrones that we used in the present work, and therefore their age determination is not completely independent from ours.

Stetson et al. (2003) derived a much older age (12 Gyr) with the help of unpublished VandenBerg isochrones. It appears that the large difference in age is due in part to the authors' choice of

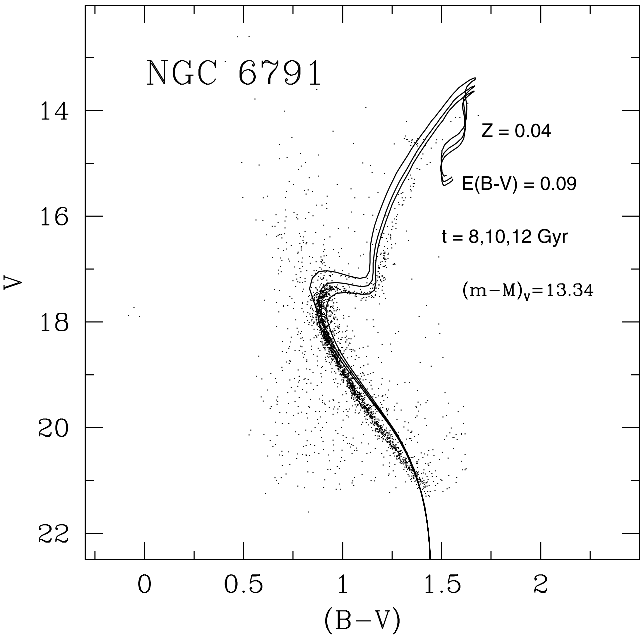

Fig. 8.—Yale-Yonsei isochrone solution for ages of 8, 10, and 12 Gyr (*from top to bottom*). Note how the two older isochrones are clearly ruled out.

a markedly smaller absolute distance modulus (12.79 mag). A superposition of the Y^2 isochrones for the range 8–12 Gyr—shifted by $(m-M)_0 = 12.79$ and $E(B-V) = 0.09$ (Stetson et al. adopted values)—on the CMD of NGC 6791 is shown in Figure 8, for comparison. Although it is not possible to rule out completely the Stetson et al. (2003) fit, the disagreement with other well-calibrated isochrones raises questions about the calibration of the VandenBerg isochrones.

An additional, independent age and distance estimate is in King et al. (2005), who obtained an excellent fit of the upper MS, TO, and SGB, both of the Stetson et al. (2003) ground-based CMD of NGC 6791 and of their *HST* ACS CMD in the F606W and F814W bands by using the Teramo isochrone set by Pietrinferni et al. (2004). From both fits, King et al. (2005) derived an age of 9 ± 1 Gyr, an absolute distance modulus $(m-M)_0 = 13.0$, and a reddening $E(B-V) = 0.12$ for a metallicity $[M/H] = +0.4$ and $Y = 0.288$. Also in the fit of the m_{F814W} versus $m_{F606W} - m_{F814W}$ *HST* ACS CMD, the Teramo isochrones tend to be redder going to fainter magnitudes, starting from $\sim$2 mag below the TO, as already noted for the Padova isochrones.

Finally, we must mention that the precise age of NGC 6791 also depends on the adopted value of the ratio $(\Delta Y/\Delta Z)$ for Galactic helium enrichment. This quantity is poorly known; it may be a function of Z and may differ from system to system. Demarque et al. (1992) have found that varying Y from 0.32 to 0.36 could reduce the age of the cluster by as much as 15%. The age estimate of NGC 6791 might have to be increased if the enrichment ratio $\Delta Y/\Delta Z$ is much less than 2 (isochrones for $\Delta Y/\Delta Z$ near 2 were assumed in the Padova, Y^2, Teramo, and VandenBerg fits).

With our present knowledge of the $\Delta Y/\Delta Z$ parameter, we conclude that the age of NGC 6791 must be in the range 7.5–8.5 Gyr, with a higher preference toward the higher limits. We point out that even in the unlikely event that the age of NGC 6791 is as low as 7.5 Gyr, its high metallicity and age present a major challenge to the accepted view of Galactic chemical enrichment.

In conclusion, three sets of independent isochrones consistently imply that the age of NGC 6791 is around 8 Gyr, adopting the metallicity and the reddening coming from observations. The difference in reddening might simply be ascribed to the different helium abundance adopted and to some photometric zero-point error.

7. DISCUSSION AND CONCLUSIONS

The most difficult issue with NGC 6791 is how, inside this cluster, such high-metallicity stars could have been produced. In fact, this cluster does not have any counterpart in the Milky Way. We note here that Kinman (1965) originally identified NGC 6791 as a globular cluster. Even if this interpretation were to be adopted, the high metallicity of NGC 6791, much higher than that of any Galactic globular cluster or nearby dwarf galaxy, remains mysterious.

With Berkeley 17 and Collinder 261, NGC 6791 is one of the oldest open clusters in the Galaxy (Carraro et al. 1999), but its metal abundance is incomparably higher. Moreover, NGC 6791 is one of the most massive open clusters (4000 $M_\odot$ at least). It lies at 1 kpc above the Galactic plane, inside the solar ring. This combination of mass and position is hard to explain, since the interaction with the dense Galactic environment should strongly depopulate a typical open cluster.

NGC 6791 is routinely considered in the studies of the chemical evolution of the Galactic disk and occupies a unique position in the Galactic disk radial abundance gradient (see Fig. 9). By including NGC 6791, the slope of the gradient changes from -0.05 (Fig. 9, *solid line*) to -0.07 (Fig. 9, *dashed line*). Besides, if one considers the slope defined only by clusters older than 4 Gyr (Friel et al. 2002; Fig. 3, *inset*), the slope doubles, from -0.06 to -0.11.

In Figure 3, the horizontal arrow indicates the epicyclical amplitude of the NGC 6791 orbit (see below, and Carraro & Chiosi 1994). One can readily see how NGC 6791 is quite an exotic object. If, by chance, at the present time the cluster would be at a different orbit phase, which would put it, e.g., beyond 12 kpc, there would be a drastic change and even an inversion of the slope of the Galactic disk abundance gradient. Finally, the position

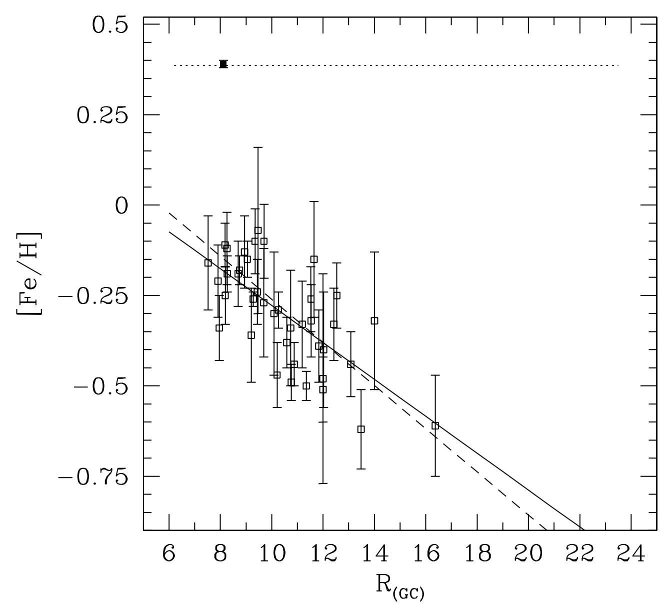

Fig. 9.—Galactic disk chemical abundance radial gradient. The data are from Friel et al. (2002), with the exception of Berkeley 22 and Berkeley 66 taken from Villanova et al. (2005) and NGC 6791 (*filled square*; coming from the present study). The solid line is the linear fit without NGC 6791, whereas the dashed line is a linear fit to all the data points. The horizontal dotted line shows the epicyclical amplitude of the NGC 6791 orbit.

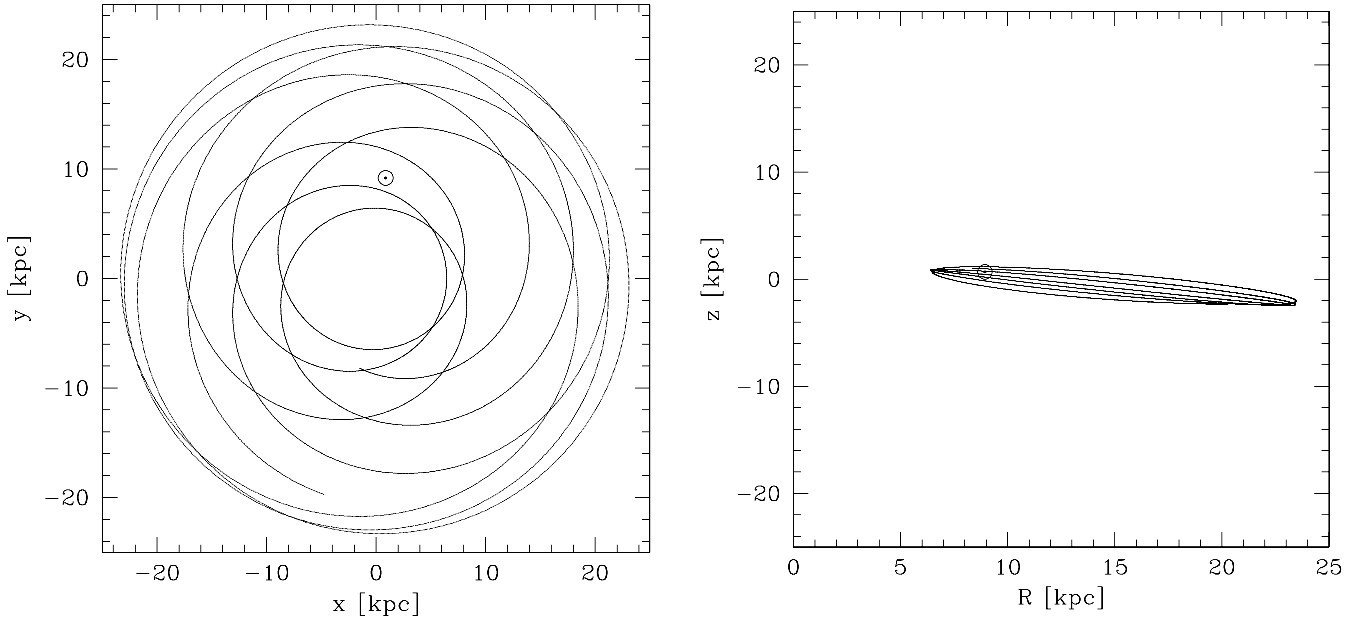

FIG. 10.—Galactic orbit of NGC 6791 in the *X-Y* and meridional plane. The position of the Sun is indicated.

of this cluster in the Galactic disk age-metallicity relationship (Carraro et al. 1998) is puzzling as well, since the cluster significantly deviates from the mean trend.

In Figure 10 we present NGC 6791's Galactic orbit. This was obtained by integrating back in time (1 Gyr) the cluster from its present position and kinematics using the Galaxy *N*-body/gasdynamical model by Fux (1997, 1999). The adopted radial velocity and proper motions come from Geisler (1988) and K. Cudworth (1999, private communication), whereas the Galactocentric rectangular initial conditions (positions and velocities) were derived as in Carraro & Chiosi (1994).

Interestingly enough, this plot shows that the cluster moves from the outer disk regions of the Milky Way, more than 20 kpc far away from the Galactic center, and enters the solar ring, going as close as 6 kpc to the Galactic center. The eccentricity ($e = 0.59$) of this orbit is quite high for a Population I star cluster (Carraro & Chiosi 1994), and it is much more similar to a globular cluster/dwarf galaxy orbit. A plausible scenario is that NGC 6791 is what remains (the nucleus) of a much larger system, which underwent strong tidal disruption. This would explain the cluster orbit and provide a reasonable explanation for the high metallicity of its stars, which could have been produced only inside a deep potential well.

However, within the observational errors, we did not find any significant abundance spread. This would mean that the bulk of the stars in the cluster was produced in a single burst of star formation. This fact makes more difficult the capture interpretation, since Local Group galaxies normally exhibit spreads in metal content and possess lower metal abundance (Mateo 1998). We stress, however, the fact that our results are based on only 10 stars and that only larger spectroscopic surveys can better address this particular problem.

An alternative, more conservative scenario is that the cluster was born in the inner side of the Galaxy, close to the bulge, where the metal enrichment has been fast. Grenon (1999) studied the kinematics of a group of old (10 Gyr) metal-rich $[\mathrm{M/H}] \geq 0.30$ stars and suggested that they formed close to the bulge and then migrated at large Galactocentric distance due to the perturbation of the Galactic bar.

The orbit we calculated actually includes the effect of the bar, and NGC 6791 indeed moves well outside the solar circle. NGC 6791 is very concentrated for an open cluster and spent most of its time at moderate Galactic latitude. This might help to explain its survival.

The observations described in this paper were carried out remotely from Yale University by Giovanni Carraro. We deeply acknowledge Diane Harmer, George Will, and Chris Hunter for support and help. The work of G. C. is supported by Fundacion Andes. G. P. and S. V. acknowledge support by the Italian MIUR, under program PRIN2003. M. V. M. is supported by an NSF Astronomy and Astrophysics Postdoctoral Fellowship, under award AST 04-011460. P. D.'s research is supported in part by NASA grant NAG5-13299.

REFERENCES

Alonso, A., Arribas, S., & Martínez-Roger, C. 1999, A&AS, 140, 261
Bedin, L. R., Anderson, J., King, I. R., & Piotto, G. 2001, ApJ, 560, L75
Bedin, L. R., Salaris, M., Piotto, G., King, I. R., Anderson, J., Cassisi, S., & Momany, Y. 2005, ApJ, 624, L45
Buson, L. M., Bertone, E., Buzzoni, A., & Carraro, G. 2006, Baltic Astron., in press (astro-ph/0509772)
Carney, B. W., Lee, J.-W., & Dodson, B. 2005, AJ, 129, 656
Carraro, G., Bresolin, F., Villanova, S., Matteucci, F., Patat, F., & Romaniello, M. 2004, AJ, 128, 1676
Carraro, G., & Chiosi, C. 1994, A&A, 288, 751
Carraro, G., Chiosi, C., Bertelli, G., & Bressan, A. 1994, A&AS, 103, 375
Carraro, G., Girardi, L., & Chiosi, C. 1999, MNRAS, 309, 430
Carraro, G., Ng, Y. K., & Portinari, L. 1998, MNRAS, 296, 1045
Chaboyer, B., Green, E. M., & Liebert, J. 1999, AJ, 117, 1360
Demarque, P., Green E. M., & Guenther, D. B. 1992, AJ, 103, 151
Demarque, P., Woo, J.-H., Kim, Y. C., & Yi, S. 2004, ApJS, 155, 667
Friel, E. D., Jacobson, H. R., Barrett, E., Fullton, L., Balachandran, A. C., & Pilachowski, C. A. 2003, AJ, 126, 2372
Friel, E. D., & Janes, K. A. 1993, A&A, 267, 75
Friel, E. D., Janes, K. A., Tavarez, M., Jennifer, S., Katsanis, R., Lotz, J., Hong, L., & Miller, N. 2002, AJ, 124, 2693
Friel, E. D., Liu, T., & Janes, K. A. 1989, PASP, 101, 1105

Fux, R. 1997, A&A, 327, 983
———. 1999, A&A, 345, 787
Garnavich, P. M., Vandenberg, D. A., Zurek, D. R., & Hesser, J. E. 1994, AJ, 107, 1097
Geisler, D. 1988, PASP, 100, 338
Girardi, L., Bressan, A., Bertelli, G., & Chiosi, C. 2000, A&AS, 141, 371
Gratton, R. G., Carretta, E., & Castelli, F. 1996, A&A, 314, 191
Green, E. M., For, B.-Q., & Hyde, E. A. 2005, in ASP Conf. Ser. 334, 14th European Workshop on White Dwarfs, ed. D. Koester & S. Moehler (San Francisco: ASP), 363
Grenon, M. 1999, Ap&SS, 265, 331
Kaluzny, J., & Rucinski, S. M. 1995, A&AS, 114, 1
King, I. R., Bedin, L. R., Piotto, G., Cassisi, S., & Anderson, J. 2005, AJ, 130, 626
Kinman, T. D. 1965, ApJ, 142, 655
Kurucz, R. L. 1992, in IAU Symp. 149, The Stellar Populations of Galaxies, ed. B. Barbuy & A. Renzini (Dordrecht: Kluwer), 225
Landsman, W., Bolihn, R. C., Neff, S. G., O'Connell, R. W., Roberts, M. S., Smith, A. M., & Stecher, T. P. 1998, AJ, 116, 789
Mateo, M. 1998, ARA&A, 36, 435
Moore, C. E., Minnaert, M. G. J., & Houtgast, J. 1996, The Solar Spectrum from 2935 to 8770 Å (Nat. Bur. Stand. Monogr.; Washington: Dept. Commerce)
Peterson, R., & Green, E. M. 1998, ApJ, 502, L39
Pietrinferni, A., Cassisi, S., Salaris, M., & Castelli, F. 2004, ApJ, 612, 168
Piotto, G., et al. 2005, ApJ, 621, 777
Ramirez, I., & Melendez, J. 2005, ApJ, 626, 465
Scott, J. E., Friel, E. D., & Janes, K. A. 1995, AJ, 109, 1706
Sekiguchi, M., & Fukugita, M. 2000, AJ, 120, 1072
Stetson, P. B., Bruntt, H., & Grundahl, F. 2003, PASP, 115, 413
Straizys, V., & Kuriliene, G. 1981, Ap&SS, 80, 353
Taylor, B. J. 2001, A&A, 377, 473
Villanova, S., Baume, G., Carraro, G., & Geminale, A. 2004, A&A, 419, 149
Villanova, S., Carraro, G., Bresolin, F., & Patat, F. 2005, AJ, 130, 652
Yi, S., Demarque, P., Kim, Y.-C., Lee Y.-W., Ree, C. H., Lejeune, T., & Barnes, S. 2001, ApJS, 136, 417